Retracking of SARAL/AltiKa radar altimetry waveforms for optimal gravity field recovery

Shengjun Zhang[1], David T. Sandwell[2]

1 School of Geodesy and Geomatics, Wuhan University, Wuhan, China

2 Scripps Institution of Oceanography, La Jolla, CA, United States

Abstract:

Keywords:

Introduction

Satellite altimetry is an effective technological means to recover marine gravity field due to its large space scale, fixed repetition frequency and relatively small cost with respect to onboard gravity metrical data. An amount of regional or global gravity field models are published in the past 40 years based on huge amount of altimeter data sets, especially these from geodetic mission phase. According to the previous analysis, the gravity filed accuracy mainly depends on range precision, spatial 2-D coverage and track orientation of altimeter. For the first factor, advanced instrument technology and improved retracking methods usually plays a huge role and is also the hot spots in the relative research area. Moreover, multi-satellites altimeter data and new geodetic mission with a longer period will meet the requirement of different track orientations and denser spatial coverage. (1.1 Gravity filed accuracy depends on range precision, 2-D coverage, and track orientation.)

As the latest launched radar altimeter, SARAL AltiKa still use conventional pulse limited mode with innovative Ka band signals of which center frequency is around 35.75GHz. The AltiKa is designed with four key innovations, which are larger bandwidth, decreased antenna beamwidth, doubled pulse repetition frequency and new echo tracking mode same as Jason2, to realize the final goal of improved range precision with a smaller footprint (Raney et al., 2011). (1.2 AltiKa is the first Ka-band altimeter.)

In detail, higher bandwidth means a smaller gate spacing of 0.31m with respect to the usual 0.47 m, which is a factor of 1.52 over flat ocean areas. Shorter wavelength

means a smaller antenna beamwidth and the footprint for AltiKa's 1-m diameter antenna from a 800km altitude will reduce to 8.9 km, in contrast to 21 km of Ku band. Additionally, decreased beamwidth increases the trailing edge decay rate and makes the measurements more statistically independent. What's more, shorter wavelength also enables sqrt(2) higher pulse repetition frequency which also enables more averaging and thus noise reduction. These improvements listed above may be expected to yield a better range precision by a factor of 2, and thereby increased the ability of constructing high precision gravity anomaly profiles. (1.3 Benefits of Ka band from Raney's paper.) (Notes: Put this part of detailed comparison in the introduction or in the following section of selecting parameters for AltiKa?)

At the opposite aspect, AltiKa has a major disadvantage as Ka band pulses are more susceptible attenuation by water droplets with respect to Ku(Raney et al., 2011). As a result, special attention should be paid to the contaminated Ka band altimeter waveforms by rain effect(Tournadre et al., 2009). (1.4 The major drawback is the Ka-band is more susceptible to water droplets than Ku-band.)

According to the previous research, AltiKa has a much lower noise level than RA-2 altimeter by more than one would expect from the ratio of pulse repetition frequency, and has an excellent performance for resolving short-wavelength geoid anomalies. As shown in the research, noise spectra show white noise floors at root-mean-square levels around 8 mm per root-Hz for AltiKa and 19 mm per root-Hz for RA2(Smith, 2015). Moreover, the retracking procedure may lead to a better performance of AltiKa. (1.5&1.6 Walter Smith compared Ka-Altika with Ku-Envisat using the standard products. He found AltiKa (50mm at 40 Hz and 8mm/sqrt(Hz)) and Envisat (80 mm at 18 Hz and 19 mm /sqrt(Hz)). Walter did not understand why there is a factor of 2 improvement because the factor of 1.52 for flat ocean should be smaller at high SWH.) (Notes: For this problem, I think a factor of 2 is achieved as a combination of higher bandwidth, higher PRF and smaller footprint.)

At the early stage when waveform retracking is firstly proposed, retracking methods will be used to improve the accuracy of data with contaminated waveforms either by sea ice or land reflective surface (Martin et al, 1983; Davis, 1995). Therefore

in the application research, retracking methods are extensively used to improve gravity field recovery at polar areas or coastal regions (Laxon et al., 1994; Hwang et al, 2006). In addition, some retracking methods can also effectively decrease the noise level of uncontaminated oceanic waveforms if special conditions are considered when modeling the waveform. As a big step for obtaining optimal recovered gravity field, a retracking method was proposed which can effectively reduces the root mean square error in the sea surface slope to only 62% percent of that of standard retracking methods(Sandwell and Smith, 2005). In the past few years, this retracking method is applied to ERS-1, Geosat/GM, Cryosat-2, Jason-1 and Envisat waveform data, and have all achieved expected effect of reduced noise level and improved gravity field recovery(Sandwell and Smith, 2009; Garcia et al., 2014). (Notes: Background of retracking.)

As a result, this paper will focus on retracking of AltiKa radar altimeter waveforms for optimal gravity field recovery and compare the range precision and resolution capability of AltiKa with previous altimeters. Envisat waveform data is selected firstly as it has exactly same repeat period, revolution numbers of each cycle and repetitive ground tracks with AltiKa. Cryosat-2 waveform data of SAR mode is also selected as they have similar waveform shapes with a faster trailing edge decay. (1.7 This study.) (Notes: Use all the altimeters for comparison? Jason-1, Cryosat-2, ERS1 and Geosat?)

Altimeter waveform theory

The conventional pulse limited radar altimeter transmits a series of frequency modulated chirp pulses with known power toward the sea surface, and recorded the received power of returned signal which have interacted with the rough sea surface. The power of returned signal depends upon the scattering character of the sea surface, the parameters of the radar system, and two-way attenuation by the intervening atmosphere. Generally, it is spatial integral of instantaneous illuminated area over the pulse-limited footprint, while the characteristic of illuminated area can be described

probabilistically by considering the average illuminated area over a hypothetical infinite ensemble of realizations.

Besides the dependence on illuminated area within the pulse limited footprint, the returned power measured by altimeter also depends on antenna gain pattern and normalized radar cross section of sea surface. However, the implementation of an automatic gain control loop in electronics package can effectively eliminates the dependence on the latter factor. As a result, the power of the returned signal is proportional to the illuminated area scaled by the off-nadir rolloff of the antenna gain pattern, which can be written by the following equations (Chelton et al., 2001).

$$W(t) = W_{\max} P_{FS}(t) * q_s(t) * p_\tau(t) \qquad (1)$$

$$P_{FS}(t) = G(t) U(t - t_{t1/2}) \qquad (2)$$

Where $q_s(t)$ is the probability density function for the sea surface height distribution, $p_\tau(t)$ is the point target response, $P_{FS}(t)$ is the radar impulse response for a flat sea surface on a spherical earth, W_{max} is the power of the average signal output by the AGC when the illuminated area becomes constant, $U(t-t_{1/2})$ is unit step function and G(t) is the two-way antenna gain pattern $G(\theta)$ with off-nadir angle θ expressed in terms of two-way travel time t. The precise form of G(t) is rather complicated and a Gaussian approximation of $G(\theta)$ takes the following form,

$$G(\theta) = G_0 \exp[-(2/\gamma)\sin^2\theta] \qquad (3)$$

$$\gamma = \frac{4}{\ln 4}\sin^2\frac{\theta_w}{2} \approx \frac{\sin^2\theta_w}{\ln 4} \qquad (4)$$

where G0 is the radar antenna boresight gain, γ is an antenna beamwidth parameter(Hayne, 1980). As a result, the trailing edge of the waveform decreases approximately exponentially with increasing two-way travel time t which is rather important for modeling altimeter waveforms.

Retracking waveform model

Retracking methods have two categories, one is based on statistics and the other involves model fitting of waveforms. According to the waveform theory in previous

section, the retracking method for optimal gravity recovery generates the model waveform through convolving the effective illuminated area with the Gaussian pulse function as equation (5). Moreover, integrating (5) using formula in Abramowitz & Stegun(1964) results in the familiar waveform model as equation (6)(Brown, 1977; Amarouche et al., 2004).

$$W(t) = A_{eff\_illu}(t) * q_s(t) * p_\tau(t) = \frac{hc}{\sigma\kappa}\sqrt{2\pi}p_0\int_{-\infty}^{\infty}\exp(\frac{-(t-t')^2}{2\sigma^2})H(t')dt' \qquad (5)$$

$$W(t) = \frac{hc\pi p_0\sqrt{2}}{\kappa}[1+erf(\eta)]\exp(-\alpha t) = \frac{A}{2}[1+erf(\frac{t}{\sqrt{2}\sigma})]\exp(-\alpha t) \qquad (6)$$

Where A is a scaling factor similar to a peak amplitude and $\eta=t/\sqrt{2}\sigma$. For our algorithm, we hold the trailing edge decay parameter α as a constant, which requires the off nadir excursions of altimeters are small enough. Additionally, the influence of background noise level is effectively eliminated through a process named waveform renormalization. Under these circumstances, there are only 3 parameters(t_0, σ, A) left for fitting waveform model and a weighted least-squares approach is used to estimate. Besides, we use an iterative mode to solve the non-linear problem in arrival time and significant wave height. The chi-squared measure of misfit is

$$\chi^2 = \sum_{i=1}^{N}[\frac{P_i - W_i(t_0,\sigma,A)}{Q_i}]^2 \qquad (7)$$

where N is the number of gates used for the fit and W_i is the modeled waveform values at the ith gate. In addition, Q_i is weight function that represents the uncertainty in the corresponding waveform power and has the following form

$$Q_i = \frac{(P_i + P_0)}{\sqrt{K}} \qquad (8)$$

where K is the number of statistically independent return echoes averaged to produce the level2 products, P_0 is power offset value which varies with the automatic gain control setting and contains the thermal noise level of instrument. Moreover, the iterative mode requires different initial estimates of fitting parameters and solves the corrected value for each parameter through the following system of linear equations:

$$\begin{bmatrix} P_1 - W_1^j \\ P_2 - W_2^j \\ \vdots \\ \vdots \\ P_N - W_N^j \end{bmatrix} = \begin{bmatrix} \frac{\partial W(t_1;t_0^j,\sigma^j,A^j)}{\partial t_0} & \frac{\partial W(t_1;t_0^j,\sigma^j,A^j)}{\partial \sigma} & \frac{\partial W(t_1;t_0^j,\sigma^j,A^j)}{\partial A} \\ \vdots & \vdots & \vdots \\ \vdots & \vdots & \vdots \\ \frac{\partial W(t_N;t_0^j,\sigma^j,A^j)}{\partial t_0} & \frac{\partial W(t_N;t_0^j,\sigma^j,A^j)}{\partial \sigma} & \frac{\partial W(t_N;t_0^j,\sigma^j,A^j)}{\partial A} \end{bmatrix} \begin{bmatrix} t_0^{j+1} - t_0^j \\ \sigma^{j+1} - \sigma^j \\ A^{j+1} - A^j \end{bmatrix} \quad (9)$$

where W_i^j means the fitting model of jth iteration, and the corresponding partial derivatives with respect to t_0, σ and A are listed as follows respectively (Garcia et al., 2014).

$$\frac{\partial W}{\partial t_0} = \frac{-A}{\sigma\sqrt{2\pi}} e^{-\eta^2} \quad (10)$$

$$\frac{\partial W}{\partial \sigma} = \frac{-A}{\sigma\sqrt{\pi}} \eta e^{-\eta^2} \quad (11)$$

$$\frac{\partial W}{\partial t_0} = \frac{W}{A} \quad (12)$$

Parameters selection for AltiKa and cmparison with Envisat

Based on the described principle, suitable parameters are chose for retracking AltiKa data and corresponding Envisat data are also used as a contrast. Firstly take the pass labeled 0002 which is almost all over the open oceans as example, the exact location for AltiKa and Envisat are plotted as the following figure. To tell them apart, the AltiKa ground track uses green thin line while the Envisat uses red thick one. As shown in figure 1, ground tracks with same orbit relative numbers are almost entirely coincident with each other for AltiKa and Envisat, which will lay a good foundation for the later contrast work.

To realize the procedure of retracking, we need to determine the data structure of AltiKa, which is still using the standard WDR structure and each 40Hz record includes 36 different items and occupies 400 bytes storage space. Compared with previous dual frequency altimeters, the parameters related to the second frequency are

replaced by rain effect parameter and retracked GDR range. (2.1 Prepare data in 40 Hz WDR structure following Jason-1 analysis. What are the major differences?)

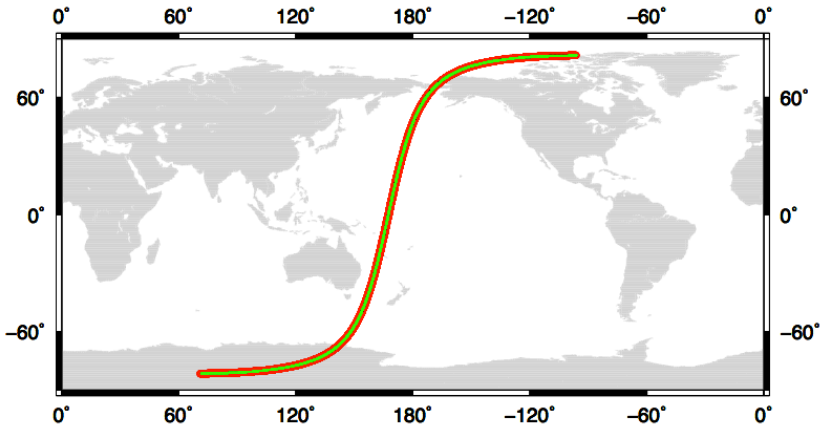

Fig1 Ground track of selected pass0002 for AltiKa(green) and Envisat(red)

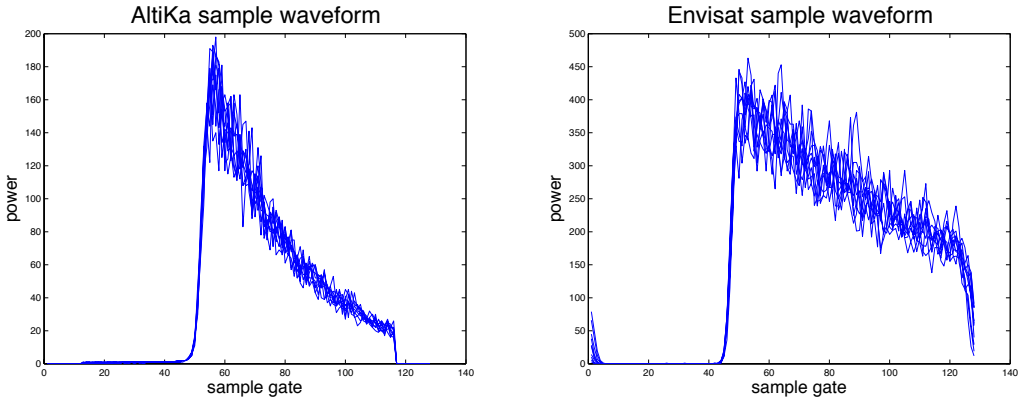

Fig2 Waveform samples of the open ocean area for Altika(left) and Envisat(right)

Take the open ocean areas for example, 10 sample waveforms of two altimeters are respectively plotted in fig2. Compared with Envisat, AltiKa has a steeper and faster trailing edge decay mainly because of the narrower antenna gain pattern. In addition, the more attenuation through wet troposphere of higher frequency and less affection by edge reflection due to the reduced footprint size may also contribute to the faster decaying trailing edge.

As mentioned in the above section, the exponential decay accounts for the antenna's gain pattern under the assumption that the 'mispointing' angle is small compared to the antenna's beam width. The AltiKa mispointing was positive around 0.003 deg^2 at the beginning of the mission, and now close to zero and extremely stable both temporally and geographically after two times of cross maneuver (Pierre Prandi, 2015). Therefore, the off-nadir excursion for AltiKa is relatively small and

does not require an alpha that depends on this angle, which means constant alpha value still works for AltiKa as previous missions. Therefore, the developed retracking method will be also suitable for AltiKa except some parameters should be adjusted or evaluated, such as gt2mm, alpha, weight function, renormalization coefficient, number of waveforms for one least-square analysis, minimum gate and maximum gate for fitting model. (2.3 Discuss pointing accuracy of SARAL so the trailing edge decay rate should not change with time)

For a given swept frequency range, sampling of spectral waveform is equivalent to "range gating" the time-domain description of the returned waveform at two-way travel time intervals δt_{eff} equal to the effective pulse duration τ which has been through pulse compression. According to the previous research, the effective two-way travel time resolution corresponding to frequency as $\delta t_{eff}=1/\Delta F$, which depends only on the chirp frequency range ΔF(Chelton,1989). As a result, the conversion parameter from gates to millimeters(gt2mm) can be written as Eq.(13). For AltiKa, the ΔF value is increased to 480MHz to improve vertical range resolution, and the gt2mm value is about 312.284 which is obviously smaller than 468.257 for Envisat.(2.2 Show detailed characteristics of waveform versus a J1 waveform. Discuss difference in gate spacing in mm as well as mingate and maxgate. (Figure 1))

$$gt2mm = \frac{c * \delta t_{eff}}{2} = \frac{c}{2 * \Delta F} \qquad (13)$$

To obtain the optimal alpha value and corresponding weight function for AltiKa, the standard deviation which is index of the misfit extent of waveform model is compared by sweeping through values of alpha at steps of 1.0e4 in an iterated manner. Based on this mode, renewed alpha value of 0.0351 is selected for AltiKa, while the alpha for Envisat is 0.009. The power offset value for weight function and renormalization coefficient don't need to modify as they adapts for AltiKa properly. Besides, the number of waveforms used for one least-square analysis also does not need to increase as the comparison shows that this modification will not improve the retracking results except with a longer time. Additionally, we use a reduced maximum gate as 75 for AltiKa which makes the solution less sensitive to alpha value and the

least squares process will run faster. Moreover, a threshold retracker is used to get a good starting location for the retracker and the threshold value uses 0.09 for AltiKa while 0.25 for Envisat. As all the parameters for AltiKa are selected, the renormalized original waveform and modeled waveform for one sample record of AltiKa and Envisat are plotted respectively. (2.4&2.5&2.6&2.7 Discuss how the trailing edge decay parameter was estimated. Discuss all other tuning and threshold retracker. Discuss why only 3 waveforms are used in the least squares at 40 Hz. Discuss 2-pass retracking method and low-pass filter used for the SWH.) (Notes: Low-filter used in creating cdr files discussed in this paper? It's a step after the retracking. By the way, I think discussion about different filter processes can be another great paper and very instructive for the students firstly trying to use altimeter data.)

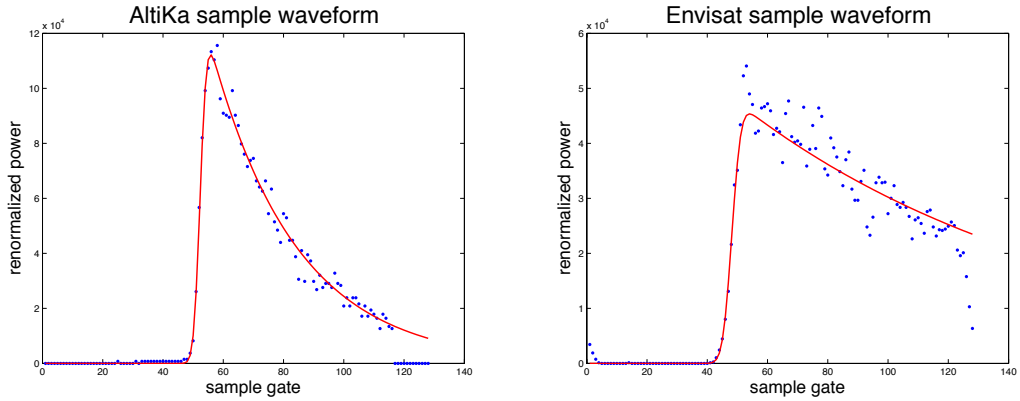

Fig3 Least-squares fit of model waveform of Altika(left) and Envisat(right)

Consideration of rain effect

As mentioned before, the main disadvantage of Ka band altimeter for AltiKa is the high sensitivity to liquid water. Therefore, one important step of our work is selecting suitable editing criteria for the retracking results and check the special parameters to indicate the rain effect. Besides, there will be two more chances to edit bad records after the retracking procedure and before we construct the grids of vertical deflection.

Suitable editing criteria for standard deviation and amplitudes will play an important role to detect the abnormal waveforms through the retracking procedure. According to the histogram analysis, the modeled amplitude should be within the

range of 150000~180000, while the chi-squared misfit measurement should be from 0 to 1500. (Notes: selection of normal range for amp and rchisq.)

In addition, the AltiKa data products provides a parameter which describes the along-track variation of estimated off-nadir angle to detect the records potentially affected by atmospheric liquid water (Tournadre et al., 2009). Generally speaking, the parameter varies along track with certain fluctuation between 60°N and 60°S, while the variation at high latitude regions is much irregular. Take the AltiKa data between 60°N and 60°S as statistical sample, an empirical choice of normal range between -0.018 and 0.0 suggested for this parameter, as a spare editing criteria. (Notes: selection of normal range for rain effect parameter(off_nadir_angle_rain_40hz).)

Noise level

To assess the noise level of AltiKa data we perform a statistical analysis on the retracked range values. Take a sample pass for each altimeter, the corresponding noise level is expressed through the standard deviation figure. Blue represents erf2 results, while green and red means erf3 and GDR results. (3.1 Present 40Hz rms about 1 Hz average for AltiKa in comparison all other altimeters (Figure 2 and Table 1))(Notes: Firstly, 1.12 is multiplied to the corresponding results. Secondly, I know the sample with only one pass is not representative, as I don't know how to select the region or cycle more convincing for the paper currently. Still use the five 40*40 region? You can give me some guidance here, dear professor.)

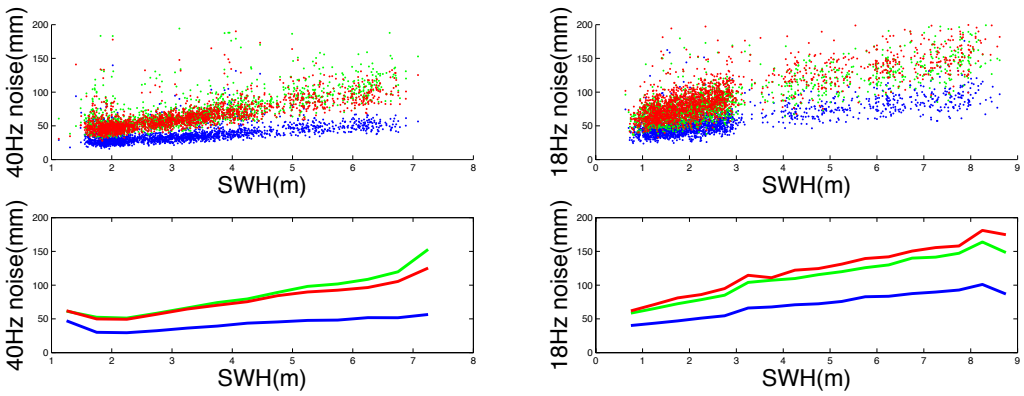

Fig4 Standard deviation of retracked height estimates with respect to EGM2008 for Altika(left) and Envisat(right)

At a typical 2m significant wave height, the mean values of standard derivation for GDR, erf3 and erf2 results is respectively 49.881mm, 52.437mm and 30.033mm for AltiKa, while 81.106mm, 72.433mm and 47.042mm for Envisat. If we statistic the records only between 60°S and 60°N, AltiKa results will be 49.720mm, 52.097mm and 29.845mm, while 81.391mm, 72.442mm and 46.971mm for Envisat. Through the comparison for the sample data, the results of 2-parameter retracking can further decrease the noise level by factor of 1.7 with respect to 3-parameter retracking for AltiKa, while the ratio is about 1.5 for Envisat. (3.2&3.3&4.4 Results show that 2-parameter retracking reduces noise by factor of 1.6 w.r.t. 3-parameter retracking. Noise level for AltiKa is only 22 mm at 20 Hz compared with > 42 mm for Ku. How do the results look in ice covered areas?) (Notes: The improvement for high latitude areas data being edited out is not apparent here because the sample is small. According to the results of whole cycle025 in notes 7, the improvement is apparent as the sea ice waveforms are more peaky as shown in my first notes 2 month ago.)

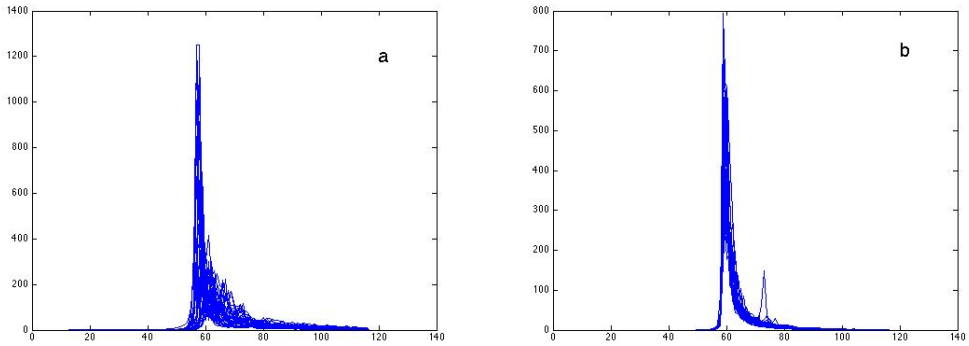

Sample waveforms for AltiKa sample pass at latitude 80N and 60N(Not used for this paper)

Coherence analysis

There is another method to evaluate the data quality of altimeter data. This methods evaluate altimeter data quality through a spectrum coherence analysis, which takes along track geoid as “signal” and the other parts of along-track sea surface height as “noise”. (3.4 Do a repeat-track cross spectral of AltiKa vs. AltiKa for a long track across the Pacific (Figure 3)) (Notes: How to realize the coherence analysis by Matlab? I previously used AR model to fit the along-track data sequences for

Cryosat-2 and plotted the power spectrum density figure, but it is very smooth and I think it definitely has some distortion to the real situation. Here is the plot example for one Cryosat-2 sample pass, which is smooth and not like the results in your papers. As a result, will you show me the rigorous way to estimate the coherence?)

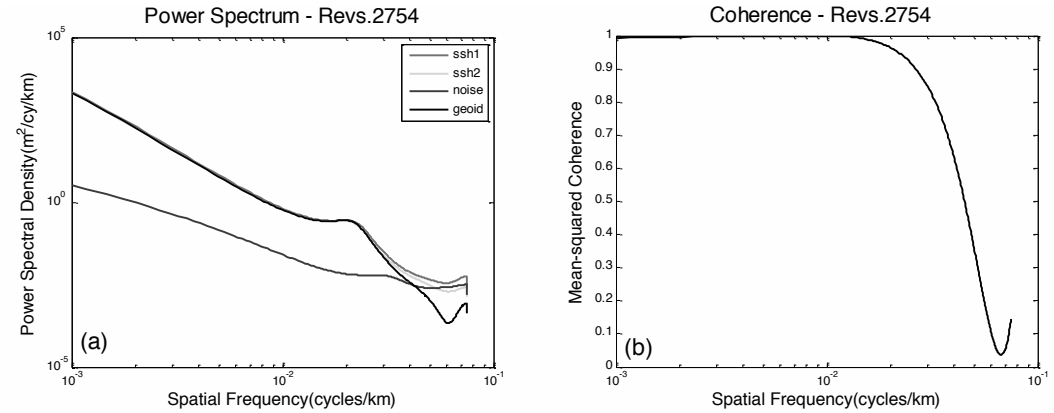

Previous result for Cryosat-2 which may mot be rigorous(Not used for this paper)

(3.5 Analysis of global map of Altika along-track slope minus slope from V23 vertical deflection grids this is filtered at 18 km 0.5 gain to match others. Show both erf3 and erf2 to examine the reduction in SWH noise (Figure 4a,b).) (Notes: I will do this work. The Figure 4a,b is just the planed figure? Any example?)

Discussion

(4.1 The double retracking provides a factor of 1.6 improvement so overall AltiKa noise is 2 X smaller than CryoSat-2 LRM noise.)

(4.2 SARAL/AltiKa drifted for a while. If the drifting orbit were continued for 3 years we would get another factor of 1.5 global gravity model improvement.)

(4.3 The noise plots shown in figure 4 have lots of data missing in the tropics because of rain)

(4.4 How do the results look in ice covered areas) (Notes: I will analyze the retracking results over ice covered areas seperately)

Conclusions

(5.1 Raney predicted a factor of 2 improvement for Ka w.r.t. K.)

(5.2 The 3-parameter retracked Ka results are 2 X better than the 3-parameter Ku.)

(5.3 This factor remains the same for double retracking.)

(5.4 Need a Ka-band altimeter in non-repeat orbit to recover seafloor features and prepare for SWOT.)

Reference

[1] Abramowitz, M & Stegun, I.A., 1964. Handbook of Mathematical Functions with Formulas, Graphs, and Mathematical Tables, U.S. Government Printing Office, Washington, D.C., 1045pp.

[2] Amarouche, L., Thibaut, P., Zanife, O.Z., et al., 2004. Improving the Jason-1 ground retracking to better account for attitude effects, Mar. Geod., 27(1-2), 171-197.

[3] Brown, G., 1977. The average impulse response of a rough surface and its applications, IEEE Transact. Antenn. Propag., 25(1), 7-74.

[4] Chelton, D.B., Edward, J.W. & MacArthurm J.L., 1989. Pulse Compression and Sea Level Tracking in Satellite Altimetry, J. Atmos. Oceanic Technol., 6, 407-438.

[5] Chelton, D.B., Ries, J.C., Haines, Fu, L.-L. & Callahan, P.S., 2001. Satellite altimetry, in Satellite Altimetry and Earth Sciences, pp. 1-131, eds. Fu, L.-L. & Cazenave, A., Academic Press.

[6] Garcia, E.S., Sandwell, D.T., Smith, W.H.F., 2014. Retracking CryoSat-2, Envisat, and Jason-1 radar altimetry waveforms for improved gravity field recovery, Geophysical Journal International, 196(3): 1402-1422.

[7] Hayne, G., 1980. Radar altimeter mean return waveforms from near-normal-incidence ocean surface scattering, IEEE Transact. Antenn. Propag., 28(5), 687-692.

[8] Hwang Cheinway, Guo Jinyun, Deng Xiaoli, et al., 2006. Coastal gravity anomalies from retracked Geosat GM altimetry: improvement, limitation and the role of airborne gravity data. Journal of Geodesy, 80(4), 204-216.

[9] Pierre Prandi, Sabine Philipps, Vincent Pignot & Nicolas Picot, 2015. SARAL/AltiKa global statistical assessment and cross-calibration with Jason-2, Marine Geodesy, DOI: 10.1080/0149 0419.2014.995840.

[10] Raney, R.K., Phalippou, L., 2011. The future of coastal altimetry, in Coastal altimetry, pp. 535-560, eds. Vingnudelli, S., et al., DOI: 10.1007/978-3-642-12796-0_20, © Springer-Verlag Berlin Heidelberg.

[11] Sandwell, D.T. & Smith, W.H.F., 2005. Retracking ERS-1 altimeter waveforms for optimal gravity field recovery, J. geophys. Int., 163(1), 79-89.

[12] Sandwell, D.T. & Smith, W.H.F., 2009. Global marine gravity from retracked Geosat and ERS-1 altimetry: ridge segmentation versus spreading rate, J. geophys. Res., 114, 1-18.

[13] Smith, W.H.F., 2015. Resolution of Seamount Geoid Anomalies Achieved by the SARAL/AltiKa and Envisat RA2 Satellite Radar Altimeters, Marine Geodesy, 38:sup1, 644-671, DOI: 10.1080/ 01490419.2015.1014950.

[14] Tournadre, J., Lambin, J. & Steunou, N., 2009. Cloud and rain effects on ALTIKA/SARAL Ka band radar altimeter, Part 1: Modeling and mean annual data availability. IEEE Transactions on Geoscience and Remote Sensing. 47(6): 1806–1817.

[15] Davis, C.H., 1995. Growth of the Greenland ice sheet: A performance assessment of altimeter retracking algorithms. IEEE Transactions on Geoscience and Remote Sensing, 33(5): 1108-1116.

[16] Martin, T.V., Zwally, H.J., Brenner, A.C., et al., 1983. Analysis and retracking of continental ice sheet radar altimeter waveforms[J]. Journal of Geophysical Research: Oceans, 88(C3): 1608-1616.

[17] Laxon, S., McAdoo, D., 1994. Arctic Ocean Gravity Field Derived From ERS-1 satellite altimetry. Science. Vol.265, No.5172: 621-624.